processes

MDPI

Article

Modification of Graphite Felt with Lead (II) Formate and Acetate—An Approach for Preparation of Lightweight Electrodes for a Lead-Acid Battery

Arminas Ilginis * and Egidijus Griškonis

Department of Physical and Inorganic Chemistry, Faculty of Chemical Technology, Kaunas University of Technology, Radvilėnų pl. 19, 50254 Kaunas, Lithuania; egidijus.griskonis@ktu.lt

* Correspondence: arminas.ilginis@ktu.lt

Received: 4 September 2020; Accepted: 28 September 2020; Published: 2 October 2020

Abstract: Lead-acid battery (LAB) weight is a major downside stopping it from being adapted to electric/hybrid vehicles. Lead grids constitute up to 50% of LAB electrode's weight and it only ensures electric connection to electrochemically active material and provides structural integrity. Using graphite felt (GF) as a current collector can reduce the electrode's weight while increasing the surface area. Modification of GF with lead (II) oxide using impregnation and calcination techniques and lead (II) formate and acetate as precursors was conducted to produce composite electrodes. It was found that lead (II) formate is not a viable material for this purpose, whereas multiple impregnation in lead (II) acetate saturated solution and calcination in air leads to thermal destruction GF. However, impregnation and calcination under nitrogen atmosphere in three cycles produced a sample of good quality with a mass loading of lead (II) oxide that was 17.18 g g^{-1} GF. This equates to only 5.5% of the total mass of composite electrode to be GF, which is immensely lower than lead grid mass in traditional electrodes. This result shows that a possible lightweight alternative of LAB electrode can be produced using the proposed modification method.

Keywords: lead-acid batteries; graphite felt; calcination; impregnation; lightweight electrodes

1. Introduction

Since its invention in 1859, Lead-acid batteries (LABs) are one of the most used rechargeable battery technologies of which the two biggest markets—automotive batteries and industrial batteries—had a ~35 BN dollar turnover in 2015 [1]. LABs are a very popular choice because of its mature technology, low cost and ability to deliver high discharge current. Almost all used LABs are recycled with recovering up to 97% of the materials used in them [2].

Traditionally LAB electrodes are made using lead or lead alloy grids, which are pasted with a mixture of leady oxide (PbO), water, sulfuric acid and additives. After immersion of lead grid electrodes, pasted with PbO, into the sulfuric acid electrolyte, the sulfation of leady oxide take place. In LABs, charge is stored and released during a fully reversible processes, by conversion of lead (II) sulphate to metallic lead and lead (IV) oxide on the negative and positive electrodes, respectively [3]:

$$PbSO_4 + H^+ + 2e^- \overset{charge \rightarrow}{\underset{\leftarrow discharge}{}} Pb + HSO_4^- \quad (1)$$

$$PbSO_4 + 2H_2O \overset{charge \rightarrow}{\underset{\leftarrow discharge}{}} PbO_2 + HSO_4^- + 3H^+ + 2e^- \quad (2)$$

A lot of effort has been put towards replacing lead alloy grids with more light-weight materials for a few reasons: they constitute up to 50% of the total weight of the electrode in LABs, they do not participate in electrochemical reactions, they only act as a current collector and they give structural strength [4]. Substitutes should have adequate mechanical strength, good corrosion resistance and

high electric conductivity [3]. The most popular choices are various types of carbon/graphite materials such as honeycombs and foams [5,6]. Furthermore, a push towards LAB applications in electric vehicles has led to a lot of research in carbon material application in LAB, mixing of carbon materials in negative active material (NAM) in particular. The addition of carbon materials in NAM increases charge-discharge cycle amount at high-rate partial state of charge and higher charge acceptance, which are crucial parameters for batteries in EV application [7–9]. More importantly, the new LAB technologies propose to completely or partially replace negative electrode with carbon materials [10]. In these batteries, carbon acts as a capacitor during charge-discharge, which alleviates stress from the negative electrode. One of the possible materials is graphite felt (GF), which is a lightweight, electrically conductive, chemically inert material [11] that has already been shown to be a great material for electrode structural base in most flow batteries [12,13] and in some types of fuel cells [14]. Electrochemical modification of GF with LAB active materials have been reported, though only with lead (IV) oxide [15], while the only non-electrochemical modification was using traditional LAB pastes [16].

The main precursor of electrochemically active material in LAB is leady oxide (mixture of lead, massicot and litharge). Traditionally, it is produced using one of two ways: the Barton pot method, in which humidified air is bubbled through molten lead to produce small particles of leady oxide, or a ball-mill process, where lead is being tumbled in a rotating mill while the collision heat allows lead to be oxidized [17]. One of the possible alternatives to traditional leady oxide is to use acetic/citric acid during recycling to leach lead from spent LAB paste to produce lead (II) acetate/citrate, which can then be calcinated at 300–450 °C to produce a mixture of lead, α and β lead (II) oxides. This would allow to omit a few steps in LAB recycling [18,19].

This work aims to investigate utilization possibility of GF as the backbone of the electrode by modifying it with lead (II) oxide-the primary electrochemically active LAB material-and to obtain lightweight LAB electrodes that require less lead. For this, first time an innovative modification methodology was attempted using impregnation with precursors-lead (II) formate and lead (II) acetate, and calcination in air and under nitrogen atmosphere. Impregnation and thermal decomposition processes, phase composition and morphology of modified GF have been analyzed and thoroughly discussed, as well as electrochemical properties of produced composite electrodes were evaluated during the charge-discharge process. The results obtained in this work show that the modification of GF with lead carboxylates, especially with acetate, presupposes a novel and promising method for the production of lightweight electrodes for LABs.

2. Materials and Methods

Square 3 cm × 3 cm size GF samples cut from a GF sheet of 4.3 × 0.2 mm thickness ("Wale Aparatus," Hellertown, Pennsylvania, USA) were used for all experiments. First, GF samples were submerged in a 20% (by volume) isopropanol ("Lachema," Brno, Czech Republic) solution to wet the surface of GF and then thoroughly washed with an excess of distilled water to remove isopropanol. A saturated aqueous solutions of lead (II) formate (puriss. p.a., "Reahim," Samara, Russia) and lead (II) acetate trihydrate (puriss. p.a., "Reahim," Samara, Russia) were prepared at 20 °C or 60 °C temperature using a "Julabo ED" thermostatic water bath. Then, individual GF samples were submerged in a saturated solution of each salt for 5 min. Impregnated GF was taken out and dried in a desiccator with $CaCl_2$ at room temperature for 12 h. The final step for all GF samples impregnated with lead (II) salts was calcination in the air, which was carried out at constant determined temperature (300, 325 or 350 °C) for 0.5–12 h. Two temperature ramps were applied: 2 °C min^{-1} (slow) or 10 °C min^{-1} (fast). Calcination was performed in muffle furnace SNOL 67/1300 with built-in temperature controller Omron®-E5CC. Additional calcinations of GF modified with lead (II) acetate were carried out under nitrogen atmosphere, which was maintained by a constant flow of 2 dm^3 min^{-1} nitrogen gas (99.996%) in muffle furnace throughout the whole calcination procedure.

X-ray diffraction (XRD) analysis of impregnated and calcined samples was done using "Bruker D8 Advance" with Cu$K\alpha$ radiation and Ni filter by using 0.02° steps that measure intensity for 0.5 s in the range from 5° to 65°.

Morphology studies were carried out with scanning electron microscopy (SEM) at various magnifications using "Hitachi S-3400N" operated at electron beam acceleration voltage of 15 kV.

Pristine and impregnated with lead (II) formate and acetate GF samples were analyzed using simultaneous thermal analysis (STA) using "Netzsch STA 409 PC Luxx" in an air atmosphere using aluminum crucibles. Temperature increase was 5 °C min^{-1} to a maximum temperature of 570 °C. Samples were prepared by crushing them with pestle and mortar and sieved to >125 μm particle size.

In some cases, the surface temperature of GF samples during calcination was measured directly in the muffle furnace using non-contact infrared thermometer "UNI-T UT301C" from a distance of about 30 cm.

Electrochemical analysis was carried out using potentiostat-galvanostat BioLogic SAS SP-150 with EC-Lab ® v10.39 software (Biolgic, Seyssinet-Pariset, France). Charging and discharging characteristics of LAB, assembled using two 2 × 1 cm produced modified GF electrodes in 38% sulfuric acid electrolyte, were analyzed using a four-step program. Firstly, the battery was charged at 50 mA until cell potential reached 2.67 V, at which point charging was complete. The battery was then left in an open circuit voltage (OCV) measuring stage for 1 h. Afterwards, the battery was discharged at a constant rate of 10 mA until the cell voltage dropped below 1.75 V. Lastly, the battery voltage was again recorded in OCV for 3 h.

3. Results and Discussion

The GF samples were weighed at different steps of modification and mass loading of lead salts on 1 g GF (after impregnation) and their solid decomposition products, mostly lead oxide (after calcination) on GFs was calculated. Table 1 illustrates that the mass increase on GF was over 5.5 times higher when lead oxide was deposited in GF matrix using saturated lead (II) acetate solution, which was prepared at 60 °C compared to 20 °C. However, there was a less dramatic change of loading when lead (II) formate solutions were used with an increase of only about 1.4 times. Furthermore, three times-repeated impregnation and calcination at 20 °C showed diminishing mass increase after each cycle compared to the first one and had lower mass increase than that of a single cycle at 60 °C for both salts. The former can be attributed to lead salt solubility in water shown in Figure 1. Lead (II) acetate has about 27 times higher solubility than lead (II) formate at 20 °C. Higher solubility allows more lead salt to accumulate inside the GF matrix during impregnation. Furthermore, solubility of lead (II) acetate polynomially increases with temperature. This leads to conditions that are more favorable to deposit a lot of precursor material in a single deposition cycle, which immensely reduces total synthesis time. However, the usage of lead (II) acetate saturated solutions at higher than 60 °C temperatures becomes complicated for impregnation processes due to the high density and viscosity of such solutions, as well as there being difficulties preparing such solutions and ensuring their stable concentration. In contrast, lead (II) formate overall showed trivial mass increases at both 20 and 60 °C and repeated impregnation and calcination, as well as that possible shedding of melted salt during the whole modification process had been significantly reducing the loading after calcination. As a result, no further modifications using lead (II) formate saturated solutions were carried out.

Table 1. The loading parameters of graphite felt (GF) samples after impregnation in saturated solution of lead (II) salts (at different temperature) and calcination at 300 °C for 1 h (temperature ramp of 2 °C min^{-1}).

Lead Salt	Temperature of Saturated Salt Solution, °C	Impregnation-Calcination Sequence No.	Loading after Impregnation, g g^{-1} GF	Loading after Calcination, g g^{-1} GF
Acetate	20	1	2.11	1.57
		2	1.36	0.64
		3	0.68	0.58
		Total	4.15	2.79
	60	1	12.6	8.90
Formate	20	1	0.18	0.13
		2	0.06	0.02

	3	0.05	0.01
	Total	0.29	0.16
60	1	0.26	0.19

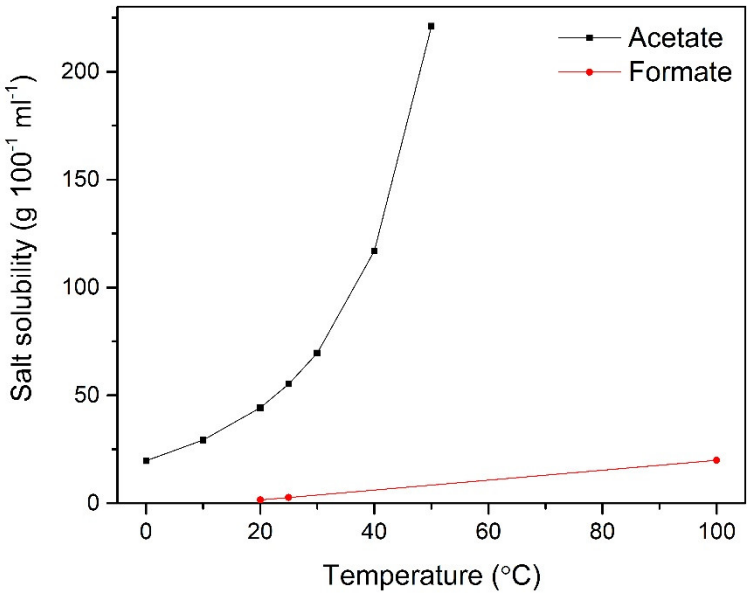

Figure 1. Solubility of lead (II) acetate and formate in water at different temperatures [20,21].

Additional experiments with different calcination algorithms were carried out in order to reduce the duration and temperature of calcination so that all of the lead (II) acetate would decompose only to α-PbO but GF would not start to burn. A ratio of mass after calcination to mass after impregnation (hereinafter referred to as the mass ratio, MR) can indicate whether all the lead (II) acetate decomposed according to such reaction scheme:

$$Pb(CH_3COO)_2 \cdot 3H_2O \xrightarrow{\Delta t} Pb(CH_3COO)_2 \xrightarrow{\Delta t} PbO \quad (3)$$

Theoretical MR, calculated according to molar masses of lead (II) oxide and lead (II) acetate hydrate, is ~0.59. This means that MR values much higher than that can indicate incomplete decomposition of lead (II) acetate. However, hypothetically, some amount of melted lead (II) acetate would run off from GF matrix during calcination; for this reason, MR is only used as a preliminary indicator of salt decomposition level which later was confirmed with XRD. As it is shown in Table 2, calcination at 300 °C is not sufficient, because MR is much higher than of those that were calcinated at 350 °C, unless duration would be lengthened to 12 h, though that would significantly increase time and energy needed for modification. Pristine GF (Figure 2a), impregnated in saturated solution of lead (II) acetate at 60 °C (Figure 2b) and calcinated at 300 °C for 12 h (Figure 2c) were completely red in color, indicating formation of only litharge (α-PbO).

After calcination at 350 °C for 1 h yellow deposits were observed on the surface of modified GFs, which indicates formation of massicot (β-PbO). Transition temperature from α to β phase is 540 °C [22], which would indicate a much higher than the set calcination temperature of 350 °C. Moreover, a physical inspection of modified GF samples that had yellow deposits showed lesser mechanical strength, which led them to disintegration from their own weight while removing from muffle furnace (Figure 2d). Lastly, small, shiny, metallic Pb microglobules were observed on the inside of disintegrated GF matrix (see SEM images below). This could be related to the carbothermal reduction of lead (II) oxide to metallic Pb, during simultaneous GF oxidation with formation mostly of gaseous carbon dioxide. The calcination at intermediate temperature of 325 °C showed that 1 h was not enough time for full decomposition, but at 2 h duration, MR was very close to MR at 350 °C. However,

an attempt of repeated impregnation and calcinations at 325 °C also showed signs of oxidative GF destruction and transition of red litharge (α-PbO) to yellow massicot (β-PbO) (Figure 2e).

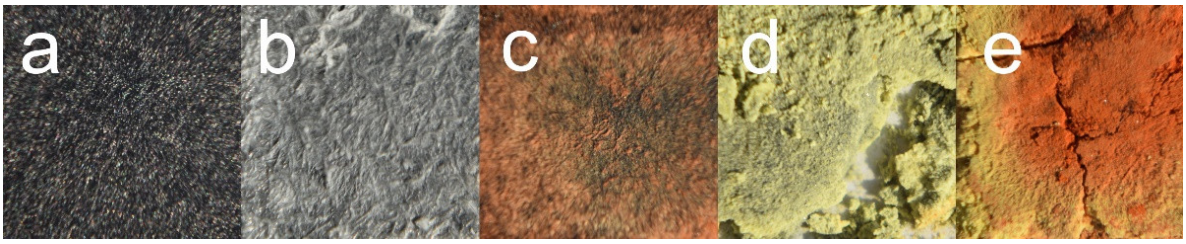

Figure 2. Photographs of GF samples: (**a**) pristine GF; (**b**) impregnated in saturated solution of lead (II) acetate at 60 °C; (**c**) impregnated with lead (II) acetate and calcinated in the air at 300 °C for 12 h; (**d**) impregnated with lead (II) acetate and calcinated in the air at 350 °C for 1 h; (**e**) impregnated with lead (II) acetate and calcinated in the air at 325 °C for 2 h, twice.

Table 2. The loading parameters of GF samples after impregnation in saturated solution of lead (II) acetate at 60 °C temperature and calcinated in the air at different temperatures and durations.

Temperature of calcination, °C	300			325		350	
Temperature ramp, °C min^{-1}	2					10	2
Duration of calcination, h	2	4	12	1	2	0.5	1
Average loading after impregnation, g g^{-1} GF	12.6						
Loading after calcination, g g^{-1} GF	8.57	8.19	7.30	8.19	6.55	7.30	6.55
MR	0.68	0.65	0.58	0.65	0.52	0.58	0.52

Therefore, an additional calcination was performed during which temperature of calcined GF sample was measured using infrared thermometer. It was obtained that maximum measured temperature reached 500 °C, which was much higher than the set temperature of 350 °C. Identical calcination was completed under an inert atmosphere of nitrogen. The GF sample's temperature during calcination process was once again measured. At that time, the observed temperature did not exceed 350 °C, indicating inhibition of exothermic runaway of GF oxidation (combustion) and left GF intact.

A hypothesis was put forward that the destruction of GF during calcination in the air would happen in three stages. First, lead (II) acetate thermal decomposition reactions, according to STA results discussed later, are exothermal and increase the temperature of GF sample over the selected temperature of 325 or 350 °C. Second, due to increased temperature GF starts to react with air oxygen forming CO, which is, once again, an exothermal reaction. In the final exothermal process, previously formed CO reacts with lead (II) oxide to reduce it to metallic lead, which itself oxidizes to CO_2. All these processes combined provide enough heat to increase the temperature of impregnated and calcined GF sample up to the measured 500 °C.

Because attempts for repeated calcination in air produced specimens with deteriorated mechanical properties as well as exothermic destruction reaction (burning) of GF substrate was observed, the calcination under an inert atmosphere was conducted. Table 3 shows that calcination experiments in N_2 atmosphere produced GF samples with lower mass compared to calcination in the air. This can be attributed to more lead (II) acetate flowing off the specimen and collecting at the bottom of the furnace during calcination. Another observation was made that thickness changed of samples from unmodified GF thickness of 4.3 to 3.5, 4.0 and 5.0 mm after first, second and third impregnations and calcination cycle, respectively. It was hypothesized that this was due to lead (II) compounds that cover GF fibers and fill the voids in between fibers. This occurrence should be noted, because increased thickness would reduce the number of electrodes that can be fitted in the LAB, which would lead to reduced energy density. Overall, a GF sample with loading up to 17.8 g g^{-1} was

obtained using repeated impregnation and calcination under inert N_2 atmosphere. It should be emphasized that in such a sample the mass fraction of GF matrix was only about 5%.

Table 3. The loading parameters of GF samples impregnated in saturated solution of lead (II) acetate salt at 60 °C temperature and calcinated at 350 °C for 30 min (temperature ramp of 10 °C min^{-1}) in the air and under nitrogen atmosphere.

Atmosphere	Air		N_2		
Impregnation-calcination sequence No.	1	2	1	2	3
Loading of lead (II) acetate, g g^{-1} GF	12.60	15.49	12.60	11.51	11.30
Loading after calcination, g g^{-1} GF	5.81	8.28	4.63	5.05	7.49
Total loading, g g^{-1} GF	14.09		17.18		

Additionally, an analysis was carried out using STA to determine at what temperature lead (II) acetate and formate completely decompose and what maximum temperature could be reached before GF starts to react with oxygen in the air. First, pristine GF sample was analyzed, which showed that GF was inert to about 400 °C. An increase in heat flow was observed, followed by a rapid mass decrease above 430 °C, which indicates ignition and combustion of GF (Figure 3, green lines).

GF sample modified with saturated lead (II) formate solution at 20 °C showed very small (due to low salt loading) exothermal peak at 275 °C, which is related to lead (II) formate decomposition to lead (II) oxide. Further increase in temperature above 400 °C led to mass decreasing, which is related to the combustion of GF (Figure 3, blue lines).

STA of the GF sample, impregnated with saturated lead (II) acetate solution at 20 °C (Figure 3. Red lines), indicated intensive endothermal process of lead (II) acetate trihydrate melting and simultaneous hydrate water release approximately at 70 °C [23]. Double endothermal peak at 170–190 °C is associated with formation of Pb $(CH_3COO)_2$ PbO. At around 280 °C, an endothermal peak of lead (II) acetate melting should appear [23]; however, this is overwhelmed by exothermic decomposition processes at 253 °C and 298 °C, which can be attributed to the formation of Pb $(CH_3COO)_2$ 2PbO. Complete decomposition to lead (II) oxide is observed at 370 °C [24].

A noteworthy observation is the onset point of GF reaction with oxygen in air, which was at a lower temperature when lead compounds were present. In addition, maximum heat flow was higher than that of pristine GF. This suggests that a reaction between lead (II) oxide and GF takes place or catalysis of GF oxidation by lead (II) oxide transpires.

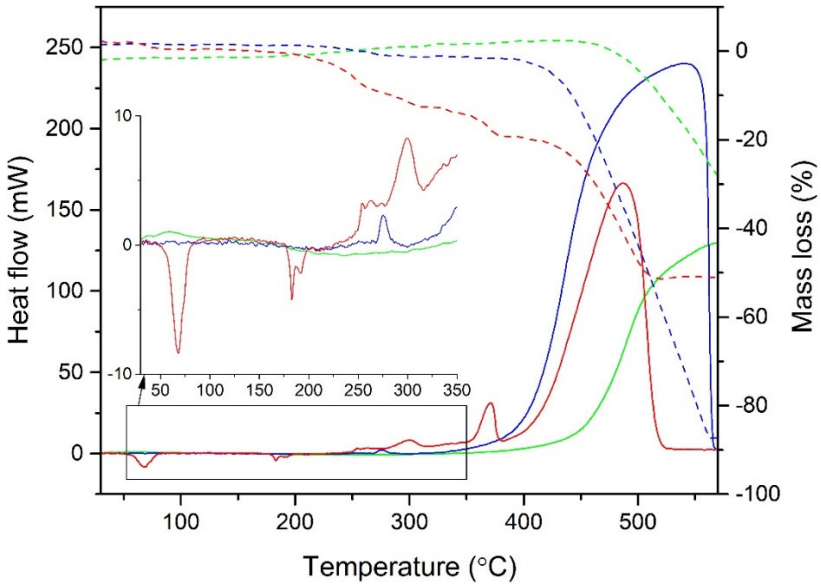

Figure 3. Simultaneous thermal analysis (STA) plot of pristine GF and modified GFs in air. Green—pristine GF, Red—GF impregnated in saturated lead (II) acetate solution at 20 °C, Blue—GF impregnated in saturated lead (II) formate solution at 20 °C. Dashed lines show mass loss %; whereas solid lines show heat flow, mW.

XRD analysis of the GF sample impregnated with lead (II) formate showed only characteristic peaks of this compound as well as broad reflection peaks of graphitic carbon (C(002) and C(002) at diffraction angles of 26° and 43°, respectively), attributed to amorphous structure of GF matrix (Figure 4). After calcination of this sample for 1 h at 300 °C, the peaks of lead (II) formate disappear and the peaks of α-PbO phase arise. This means that calcination at 300 °C for 1 h was enough for full decomposition of lead (II) formate and confirms the data of STA.

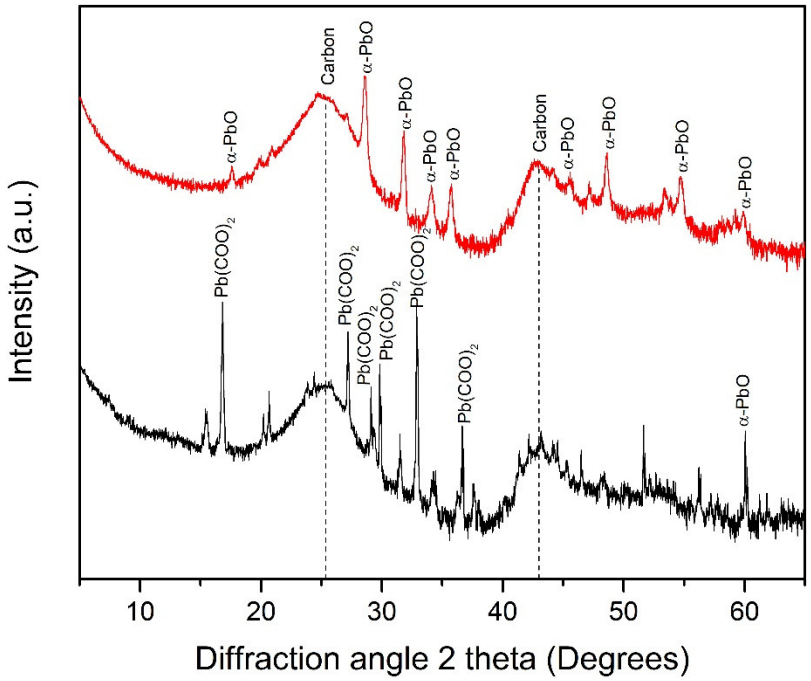

Figure 4. X-ray diffraction (XRD) patterns of GF modified with lead (II) formate (black) at 20 °C and after calcination at 300 °C for 1 h (red).

The XRD patterns of GF samples impregnated with saturated lead (II) acetate solution at 60 °C and dried, as well as calcined at different conditions, are shown in Figure 5. The impregnated and dried GF sample shows characteristic peaks of the mixture of anhydrous and hydrated lead (II) acetate phases (Figure 5). After calcination at 300 °C with durations of 1 h the peaks of lead (II) acetate were still observed, while the characteristic peaks of α-lead (II) oxide and basic lead (II) acetate are also identified (Figure 5). If the duration of calcination is increased to 12 h, the characteristic peaks of lead (II) acetate disappear, yet the peaks of α and β lead (II) oxides become more intense (Figure 5). It should be emphasized that all of the XRD patterns of samples modified with lead (II) acetate lack broad peaks that are of graphitic carbon. This indicates significant coverage of GF fibers with lead compounds, which shield GF from x-rays.

Increasing temperature to 325 °C yields results with primarily intense peaks of α-lead (II) oxide and low peaks of β-lead (II) oxide (Figure 5). Even though previously mentioned weight ratio of sample after 1 h showed higher value than other samples and it was hypothesized that full decomposition did not occur. Meanwhile, samples calcinated at 350 °C showed full decomposition of lead (II) acetate to both α and β phases of lead (II) oxide (Figure 5). When nitrogen atmosphere was maintained during calcination, only α phase of lead (II) oxide is observed (Figure 5), although according to the literature some metallic lead peaks should also appear [24]. However, the peaks attributed to the metallic phase of lead, in this case, were not observed.

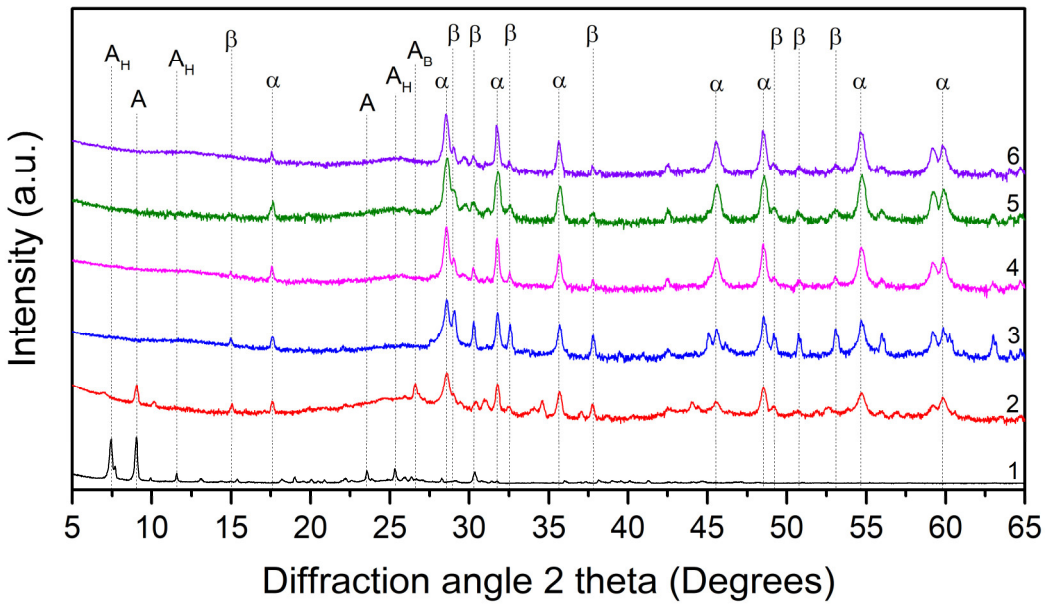

Figure 5. XRD patterns of GF samples impregnated with saturated lead (II) acetate solution at 60 °C and after that calcinated at different temperatures and durations. Here: 1—impregnated and dried; 2—300 °C 1 h; 3—300 °C 12 h; 4—325 °C 1 h; 5—350 °C 1 h; 6—350 °C 0.5 h under N_2. Here: A_H—$Pb(CH_3COO)_2\ 3H_2O$, A—$Pb(CH_3COO)_2$, A_B—$Pb(CH_3COO)_2\ 2PbO$, α—α-PbO, β—β-PbO.

The SEM analysis showed that fibers of pristine GF (Figure 6a) after impregnation with lead (II) acetate are almost completely covered in elongated and small crystals (Figure 6b). On the other hand, after calcination ordered crystalline structure changed to irregular shapes, voids and spikes that increase the surface area and is beneficial for electrochemical processes (Figure 6c). This was most likely caused by gaseous decomposition products such as CO_2. GF impregnated with lead (II) formate showed much smaller and far fewer crystals (Figure 6d,e) compared to acetate (Figure 6b,c), which agrees with loading values discussed previously.

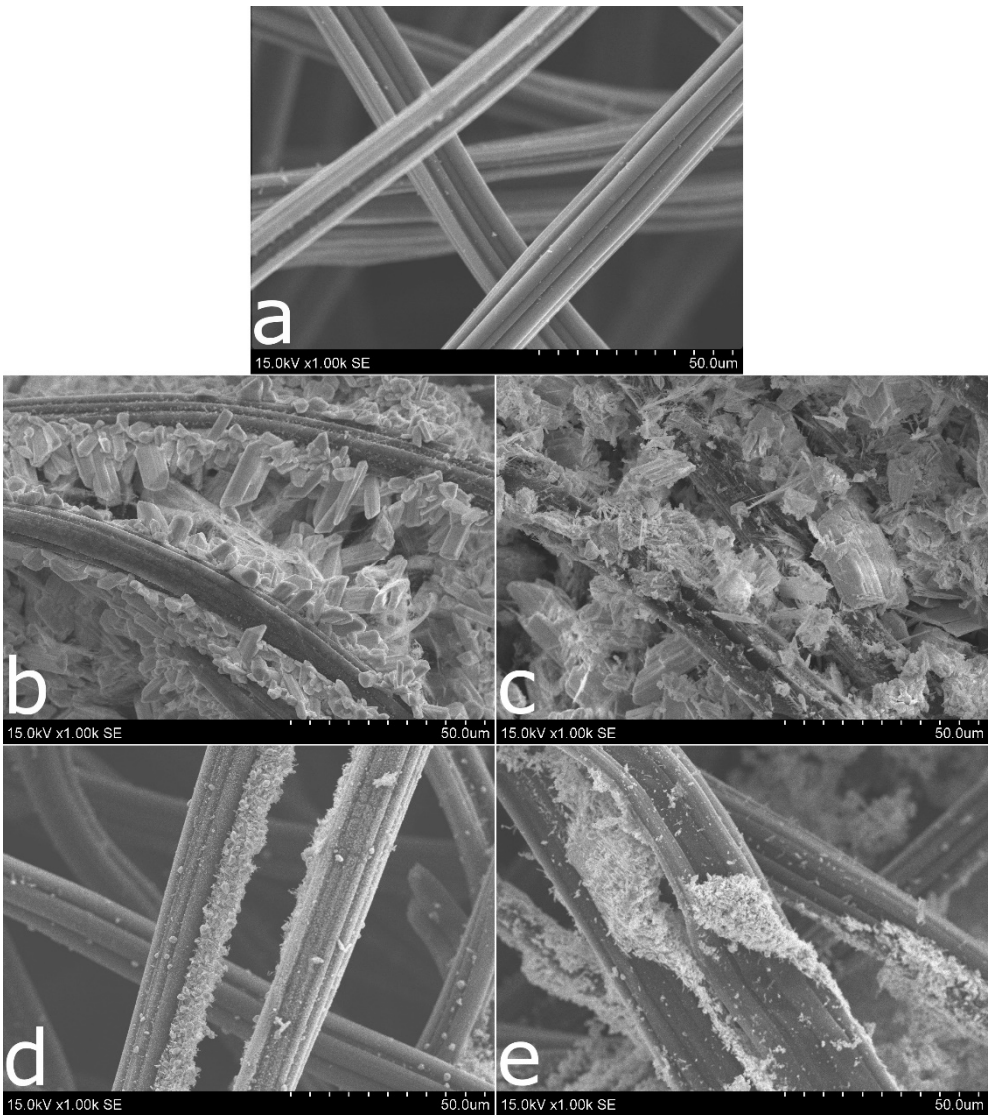

Figure 6. SEM images of GF samples at different modification conditions: (**a**) pristine GF; (**b**) GF impregnated with saturated lead (II) acetate solution at 60 °C; (**c**) GF impregnated with saturated lead (II) acetate solution at 60 °C and calcinated in 300 °C for 1 h (temperature ramp 2 °C min^{-1}); (**d**) GF impregnated with saturated lead (II) formate solution at 60 °C; (**e**) GF impregnated with saturated lead (II) formate solution at 60 °C in 300 °C for 1 h (temperature ramp 2 °C min^{-1}).

The SEM image of GF impregnated in 60 °C lead (II) acetate saturated solution and calcinated at 350 °C in air is presented in Figure 7a. In this sample, GF fiber coverage with lead (II) oxide is sparse and minimal void filling between fibers is observed. Investigation of the GF sample, which was repeatedly impregnated in 60 °C lead (II) acetate saturated solutions and calcinated at 350 °C in air, showed loss of mechanical strength and yellow deposit, as well as demonstrated mostly aggregates of metallic Pb microglobules and, in some areas, scaly morphology, which were completely different from ones previously observed (Figure 7b,c). Furthermore, only remnants of GF fibers in form of short segments can be seen. It is an obvious sign of GF matrix destruction.

SEM images of repeated GF impregnated in 60 °C lead (II) acetate saturated solutions and calcinated at 350 °C under nitrogen atmosphere show increasing coverage of GF fibers after each cycle (Figure 7d,f) and show no GF matrix destruction signs. Even after the second cycle, fibers of GF are almost completely covered in lead (II) oxide crystals, whereas voids between fibers are almost completely filled with lead (II) oxide.

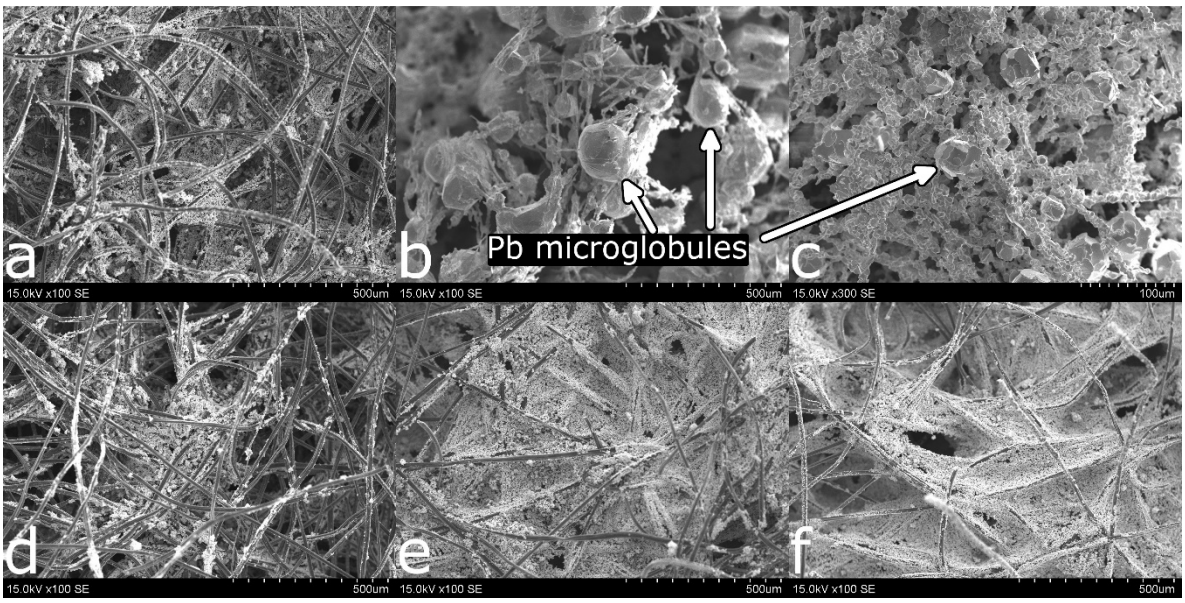

Figure 7. SEM images of GF impregnated with saturated lead (II) acetate solution at (**a–c**) 60 °C and calcinated in the air and (**d–f**) under nitrogen at 350 °C for 0.5 h (temperature ramp 10 °C min^{-1}). Here: (**a**) after the first cycle of impregnation and calcination in the air; (**b,c**) after the second impregnation and calcination cycle in the air at different spots and magnifications; (**d–f**) after the first, the second and the third impregnation and calcination cycle under nitrogen, respectively.

Comparing SEM images of the outside and inside of GF samples that were calcinated in air shows different morphologies of formed crystals (Figure 8a,b). Crystal size on the inside is significantly smaller than that of the outside, which means an increase in surface area. Higher surface area is desired because this would increase maximum capacity as well as charging-discharging rate. This difference could be due to higher temperature inside of the GF matrix than on the outside fibers. Comparing samples obtained after firs impregnation-calcination cycle in the air and under nitrogen atmosphere show no significant differences (Figure 8c,d). In both cases the formed crystals are small (< 1 μm) and form porous agglomerates. Some pores between them go down to GF fibers.

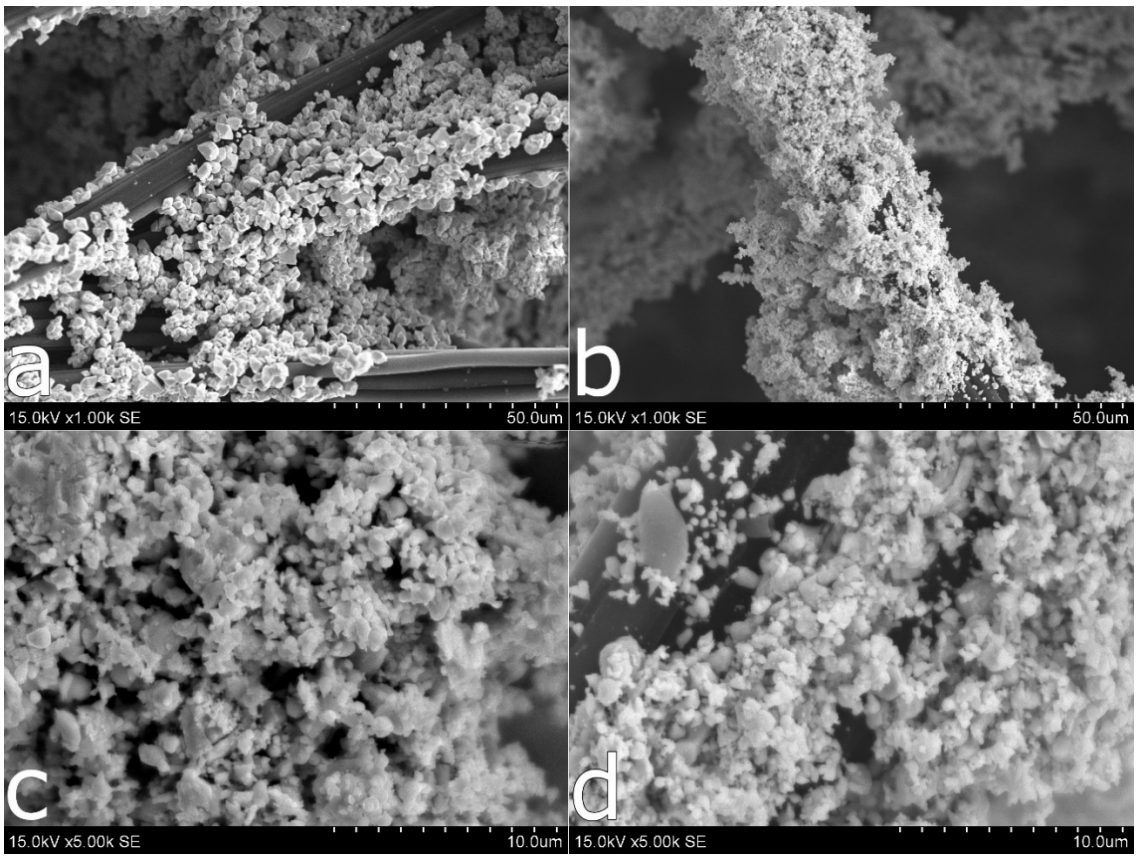

Figure 8. SEM images of GF samples impregnated with saturated lead (II) acetate solution at 60 °C and calcinated at 350 °C for 0.5 h (temperature ramp 10 °C min^{-1}) under different atmospheres: (**a**) outside of the GF calcinated under air atmosphere at 1000× magnification, (**b**) inside of the GF calcinated under air atmosphere at 1000× magnification, (**c**) inside of the GF calcinated under air atmosphere at 5000× magnification, (**d**) inside of the GF calcinated under nitrogen atmosphere at 5000× magnification.

Produced composite electrodes after three-time impregnation in saturated lead (II) acetate solution at 60 °C and calcinated at 350 °C under nitrogen atmosphere were used to construct a battery and to test its capacity (Figure 9). Firstly, chemical and electrochemical formation of the battery's electrodes was performed. It consisted of soaking the electrodes for 4 h in sulfuric acid electrolyte to convert lead (II) oxide to basic lead (II) sulfate and then passing current through the system to convert lead (II) oxide to metallic lead and lead (IV) oxide on cathode and anode, respectively:

$$4PbO + H_2SO_4 \rightarrow 3PbO \cdot PbSO_4 \cdot H_2O \quad (4)$$

$$3PbO \cdot PbSO_4 \cdot H_2O + 4H_2O \rightarrow 4PbO_2 + HSO_4^- + 8e^- + 9H^+ \quad (5)$$

$$3PbO \cdot PbSO_4 \cdot H_2O + 7H^+ + 8e^- \rightarrow 4Pb + HSO_4^- + 4H_2O \quad (6)$$

During charging of the battery from a discharged state, a total of 214.6 mAh of charge had passed through before the cell voltage reached 2.67 V, at which point lead (II) sulfate conversion to lead and lead (IV) oxide on cathode and anode respectively stopped, indicating charging was complete.

After an hour in OCV mode, the battery voltage stabilized at 2.15 V. During discharge at a constant load of 10 mA, cell voltage steadily declined and had a sharp drop after almost 17 h, indicating the end of discharging. From the discharge data, a battery capacity of 169.2 mAh was calculated, whereas the charge efficiency of the battery was 78.8%. Maximum theoretical battery capacity was determined according to deposited amount of lead (II) oxide on GF to be 487.5 mAh. This amounts to only 34.7% of electrochemically active material participating during discharge. The later could be attributed to the composite electrode's three-dimensional structure. Using a thinner GF

substrate could allow the innermost electrochemically active materials to have better participation during charging and discharging.

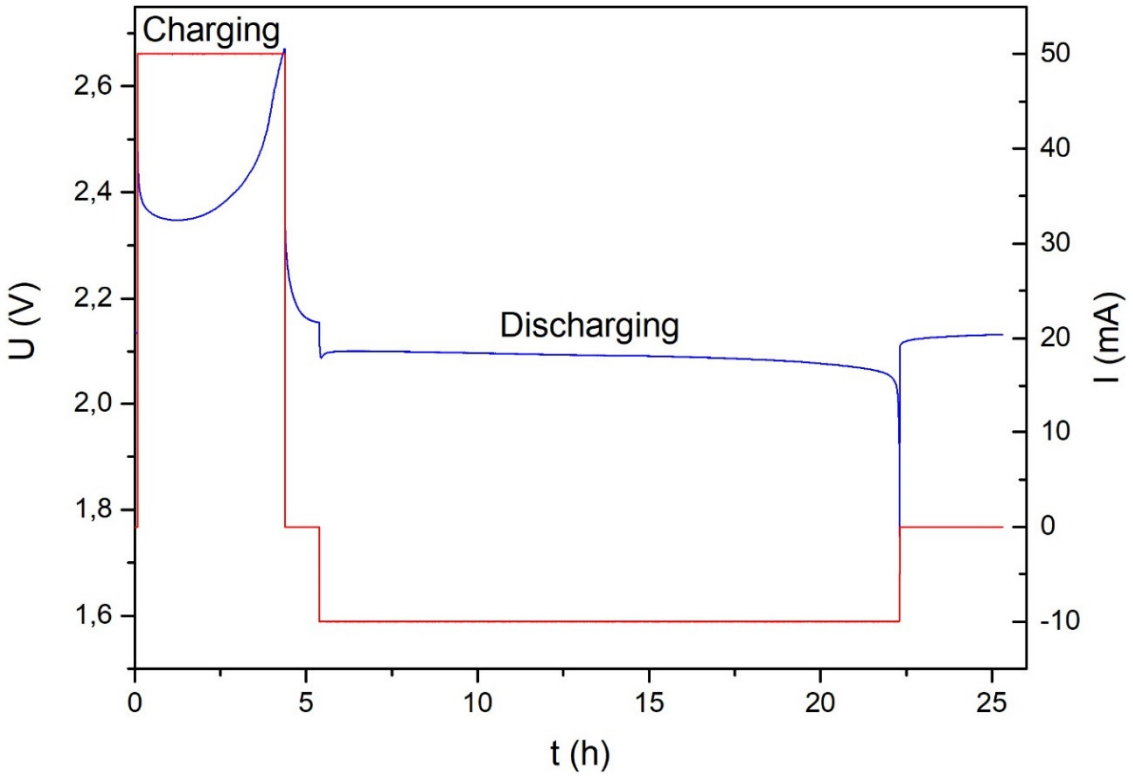

Figure 9. Voltage (blue) and current (red) change in lead-acid batteries (LABs) made from GFs three times impregnated in saturated lead (II) acetate solution and calcinated under nitrogen atmosphere in 350 °C for 0.5 h electrodes in 38% sulfuric acid electrolyte.

4. Conclusions

The results show that in order to produce samples with highest loading and repeated cycles, impregnation should be carried out in saturated solutions of lead (II) acetate at 60 °C. Calcination should be completed at 350 °C to reduce the time required for full decomposition of lead (II) acetate and necessarily under nitrogen atmosphere, because such calcination in air would produce burned samples with no mechanical strength. Under these conditions, the sample with loading of lead (II) oxide up to 17.18 g g^{-1} graphite felt was produced. At this loading the mass of graphite felt equates to only 5.5% of the total mass of composite electrode. Such mass of graphite felt matrix is significantly lower than lead grid mass in a traditional electrode, which can be up to 50%. In comparison, modification of graphite felt by using lead (II) formate produced samples with miniscule loading of lead (II) oxide (1.19 g g^{-1} graphite felt). This means that lead (II) formate is not suitable for high mass loading applications such as battery electrodes.

Electrochemical analysis proved that produced composite electrodes can be used as a LAB electrode with a specific capacity of 78.7 mAh g^{-1} or 78.7 Ah kg^{-1} for a single electrode.

The produced electrodes would allow not only for the lead-acid battery to have a higher energy density, but would require less lead, as well as reduced demand for lead ore, substituting it for recycled lead and its compounds.

Measures to reduce expansion after repeated impregnation and calcination of modified graphite felt samples should be investigated to increase density. Further optimization of modification parameters could lead to a reduction of mass shedding during calcination, enhanced crystalline structure, lower energy and time cost.

Author Contributions: Conceptualization, methodology and writing—review and editing, E.G.; conceptualization, investigation and writing—original draft, A.I. All authors have read and agreed to the published version of the manuscript.

Funding: This research received no external funding.

Conflicts of Interest: The authors declare no conflict of interest.

Abbreviations

LAB	lead-acid batterie(s)
GF	graphite felt
NAM	negative active material
XRD	X-ray diffraction
SEM	scanning electron microscopy
STA	simultaneous thermal analysis
OCV	open circuit voltage
MR	mass ratio

References

1. May, G.J.; Davidson, A.; Monahov, B. Lead batteries for utility energy storage: A review. *J. Energy Storage* **2018**, *15*, 145–157, doi:10.1016/j.est.2017.11.008.
2. Ballantyne, A.D.; Hallett, J.P.; Riley, D.J.; Shah, N.; Payne, D.J. Lead acid battery recycling for the twenty-first century. *R. Soc. Open Sci.* **2018**, *5*, 171368, doi:10.1098/rsos.171368.
3. Pavlov, D. *Lead-Acid Batteries: Science and Technology*, 2nd ed.; Elsevier: Amsterdam, The Netherlands, 2017; ISBN 978-0-444-59552-2.
4. Kirchev, A.; Kircheva, N.; Perrin, M. Carbon honeycomb grids for advanced lead-acid batteries. Part I: Proof of concept. *J. Power Sources* **2011**, *196*, 8773–8788, doi:10.1016/j.jpowsour.2011.06.021.
5. Czerwiński, A.; Wróbel, J.; Lach, J.; Wróbel, K.; Podsadni, P. The charging-discharging behavior of the lead-acid cell with electrodesbased on carbon matrix. *J. Solid State Electrochem.* **2018**, *22*, 2703–2714, doi:10.1007/s10008-018-3981-4.
6. Chen, Y.; Chen, B.Z.; Ma, L.W.; Yuan, Y. Effect of carbon foams as negative current collectors on partial-state-of-charge performance of lead acid batteries. *Electrochem. Commun.* **2008**, *10*, 1064–1066, doi:10.1016/j.elecom.2008.05.009.
7. Moseley, P.T.; Rand, D.A.J.; Davidson, A.; Monahov, B. Understanding the functions of carbon in the negative active-mass of the lead-acid battery: A review of progress. *J. Energy Storage* **2018**, *19*, 272–290, doi:10.1016/j.est.2018.08.003.
8. Pavlov, D.; Nikolov, P. Capacitive carbon and electrochemical lead electrode systems at the negative plates of lead–acid batteries and elementary processes on cycling. *J. Power Sources* **2013**, *242*, 380–399, doi:10.1016/j.jpowsour.2013.05.065.
9. Enos, D.G.; Ferreira, S.R.; Barkholtz, H.M.; Baca, W.; Fenstermacher, S. Understanding function and performance of carbon additives in lead-acid batteries. *J. Electrochem. Soc.* **2017**, *164*, 3276–3284, doi:10.1149/2.1031713jes.
10. Moseley, P.T.; Rand, D.A.J.; Peters, K. Enhancing the performance of lead–acid batteries with carbon–In pursuit of an understanding. *J. Power Sources* **2015**, *295*, 268–274, doi:10.1016/j.jpowsour.2015.07.009.
11. Castañeda, L.F.; Walsh, F.C.; Nava, J.L.; de León, C.P. Graphite felt as a versatile electrode material: Properties, reaction environment, performance and applications. *Electrochim. Acta* 2017, *258*, 1115–1139, doi:10.1016/j.electacta.2017.11.165.
12. Leung, P.; Li, X.; de León, C.P.; Berlouis, L.; Low, C.T.J.; Walsh, F.C. Progress in redox flow batteries, remaining challenges and their applications in energy storage. *RSC Adv.* **2012**, *27*, 10,125–10,156, doi:10.1039/C2RA21342G.
13. Zhang, W.; Xi, J.; Li, Z.; Zhou, H.; Liu, L.; Wu, Z.; Qiua, X. Electrochemical activation of graphite felt electrode for VO2+/VO2+ redox couple application. *Electrochim. Acta* **2013**, *89*, 429–435, doi:10.1016/j.electacta.2012.11.072.
14. Flimban, S.G.A.; Ismail, I.M.I.; Kim, T.; Oh, S. Overview of recent advancements in the microbial fuel cell from fundamentals to applications: Design, major elements, and scalability. *Energies* **2019**, *12*, 3390–3410, doi:10.3390/en12173390.

15. Mo, H.; Tang, Y.; Wang, X.; Liu, J.; Kong, D.; Chen, Y.; Wan, P.; Cheng, H.; Sun, T.; Zhang, L.; et al. Development of a three-dimensional structured carbon fiber felt/β-PbO2 electrode and its application in chemical oxygen demand determination. *Electrochim. Acta* **2015**, *176*, 1100–1107, doi:10.1016/j.electacta.2015.07.126.
16. Christie, S.; Wong, Y.S.; Titelman, G.; Abrahamson, J. Lead-Acid Battery Construction. U.S. Patent 9,543,589 B2, 10 January 2017.
17. Dix, J.E. A comparison of barton-pot and ball-mill processes for making leady oxide. *J. Power Sources* **1987**, *19*, 157–161, doi:10.1016/0378-7753(87)80024-1.
18. Hu, Y.; Yang, J.; Zhang, W.; Xie, Y.; Wang, J.; Yuan, X.; Kumar, R.V.; Liang, S.; Hu, J.; Wu, X. A novel leady oxide combined with porous carbon skeleton synthesized from lead citrate precursor recovered from spent lead-acid battery paste. *J. Power Sources* **2016**, *304*, 128–135, doi:10.1016/j.jpowsour.2015.11.030.
19. Sun, X.; Yang, J.; Zhang, W.; Zhu, X.; Hu, Y.; Yang, D.; Yuan, X.; Yu, W.; Dong, J.; Wang, H.; et al. Lead acetate trihydrate precursor route to synthesize novel ultrafine lead oxide from spent lead acid battery pastes. *J. Power Sources* **2014**, *269*, 565–576, doi:10.1016/j.jpowsour.2014.07.007.
20. Rabinovich, V.A.; Havin, Z.Y. *A Brief Chemical Handbook*; Khimiya: Leningrad, Russia, 1978; p. 94. (In Russian)
21. De Vekki, D.A.; Moskvin, A.V.; Yetrov, M.L.; Reznikov, A.N.; Skvortsov, N.K.; Trishin, Y.G. *New Handbook of Chemist and Technologist. Basic Properties of Inorganic, Organic and Organo-Elemental Compounds*; Mir i Semja: Sankt-Peterburg, Russia, 2007, p. 272. (In Russian)
22. Adams, D.M.; Christy, A.G.; Haines, J. Second-order phase transition in PbO and SnO at high pressure: Implications for the litharge-massicot phase transformation. *Phys. Rev. B* **1992**, *46*, 11358–11367, doi:10.1103/PhysRevB.46.11358.
23. Haynes, W.M. *Handbook of Chemistry and Physics*; 96th ed. CRC Press: Boca Raton, FL, USA, 2015 (Internet Version 2016); ISBN 9781482260960.
24. Casado, F.J.M.; Riesco, M.R.; Cheda, J.A.R.; Cucinotta, F.; Matesanz, E.; Miletto, I.; Gianotti, E.; Marchese, L.; Matěj, Z. Unraveling the decomposition process of lead(II) acetate: Anhydrous polymorphs, hydrates, and byproducts and room temperature phosphorescence. *Inorg. Chem.* **2016**, *55*, 8576–8586, doi:10.1021/acs.inorgchem.6b01116.